European Journal of Cardio-Thoracic Surgery 43 (2013) 829–838
doi:10.1093/ejcts/ezs388 Advance Access publication 5 July 2012

ORIGINAL ARTICLE

A computational fluid dynamics study on geometrical influence of the aorta on haemodynamics

Kwong Ming Tse[a,*], Rong Chang[a], Heow Pueh Lee[a], Siak Piang Lim[a], Sudhakar Kundapur Venkatesh[b] and Pei Ho[c]

[a] Department of Mechanical Engineering, National University of Singapore, Singapore
[b] Department of Diagnostic Radiology, National University Hospital, Singapore
[c] Department of Cardiac, Thoracic & Vascular Surgery, National University Hospital, Singapore

* Corresponding author. Department of Mechanical Engineering, National University of Singapore, 9 Engineering Drive 1, Singapore 117576. Tel: +65-65-168934; fax: +65-67-791459; e-mail: tsekm.research@yahoo.com or g0900558@nus.edu.sg (K.M. Tse).

Received 6 February 2012; received in revised form 22 May 2012; accepted 30 May 2012

Abstract

OBJECTIVES: Cardiovascular diseases, such as atherosclerosis and aneurysm, are closely associated with haemodynamic factors that are governed by luminal geometry. The present work aimed to study the effect of geometrical variation of aging aortas on haemodynamics.

METHODS: Six aged subjects with intricate geometrical features, such as bulging or twisted supra-aortic arteries, sharply curved arch and double-curved descending aorta, were chosen from our medical database. These six geometrically variant aortas were reconstructed and the pulsatile nature of the blood flow of these subject-specific aorta models investigated using computational fluid dynamics simulations. Realistic time-dependent boundary conditions are prescribed for various arteries of the aorta models.

RESULTS: This study suggests that haemodynamics in the human aorta is highly dependent on geometrical features. The positioning and contouring of the supra-aortic arteries may be associated with the skewness of velocity profiles. The flow profiles in the aortic arch or bends are generally skewed towards the inner curvature wall and this skewness may give rise to the formation of secondary flow in the inner curvature wall of the distal arch. The degree of vorticity in the distal aortic arch is found to be related to the arch curvature. The helical nature of aortic haemodynamics is predominant in the systole phrase when it begins with a left-handed rotation and then vanishes in the ascending aorta, whereas a right-handed rotation persists in the distal aortic arch. Lower wall shear stress is also found in the ascending regions where secondary flow is present.

CONCLUSIONS: The aorta with an irregular contour and large degree of curvature at its arch favours the development of the intra-aortic secondary flow that subsequently relates to the pathogenesis of atheroma. The present study identifies the general trend of haemodynamic behaviours associated with various local geometrical features. Combining the knowledge of the correlation between haemodynamics and the underlying risks in the development of cardiovascular diseases, our study hopes to provide a better understanding of the relationship between aortic morphology and developing pathobiology of cardiovascular diseases. As such, early medical planning as well as surgical interventions can be designed to retard or prevent the development of cardiovascular diseases.

Keywords: Geometrical influence • Haemodynamics • Aging aorta • S-shaped descending aorta • Supra-aortic arteries • Computational fluid dynamics (CFD)

INTRODUCTION

It is well recognized that cardiovascular diseases, such as atherosclerosis and aneurysm, are closely associated with haemodynamic factors that are governed by luminal geometry. Geometrical complexities in the human aorta, as illustrated by the presence of non-planar curvatures, supra-aortic branches and significant tapering of the aortic wall, give rise to complications in haemodynamic behaviours, thus making the aorta one of the most vulnerable arteries for possible development of cardiovascular diseases [1, 2]. In the past decade, the correlation of haemodynamics and cardiovascular diseases had been fairly understood [2]. Numerous computational and experimental studies had indicated the correlation of haemodynamic parameters such as wall shear stress (WSS) and flow variables with initiation and progression of atherosclerotic plaques and aneurismal diseases [2]. However, little is known about the influence of arterial geometry on haemodynamics with relatively less focus on local effects of arterial geometry. The earlier computational studies had undoubtedly provided the first insight on the effect of arterial geometry on haemodynamics [1, 3]. Nonetheless, they had made numerous approximations and simplifications in the

aortic geometry. One of these was the approximation of the aorta as a smooth curved tube with a fixed cross-sectional area [1, 3]. Such simplifications failed to capture intricate geometrical details, hence lost insight on their manifestation in the unpredictable flow pattern due to the aortic geometry [4].

Various techniques in imaging and numerical computation have been employed since a few decades ago. Numerical approaches, in particular, those which are capable of obtaining haemodynamic parameters non-invasively, have been used extensively. In recent years, image-based computational fluid dynamics (CFD) has emerged as a practical tool for investigating haemodynamics, and there is an emerging trend of analysing aorta models reconstructed from *in vivo* imaging data [5, 6]. These image-based CFD studies achieved the elimination of the above-mentioned simplifications by having realistic arterial geometry. Unfortunately, they were often limited in the selections of models that did not display significant geometrical variations from the ideal candy cane shape. Since an aorta of older age was reported to have larger radius of curvature with increased centerline length (question mark shaped) [4], which can be associated with the increasing risk of developing cardiovascular diseases in old age, these studies with candy cane shaped aortas failed to represent that of the older population. The present study attempts to examine subject-specific aortas with distinct anatomical features and aims to provide a more comprehensive study of geometrical variation of aorta due to old age on fluid dynamics behaviour. With methodical examination, this promises a better insight on the aorta's geometrical influence.

MATERIALS AND METHODS

Reconstruction from computed tomography imaging

Six geometrically variant models of subjects with an age range of 54–72 (mean = 60.8 and SD = 5.1) chosen from our medical database of 75 subjects (mean = 66.5 and SD = 10.4) were examined. This medical database consisted of computed tomography (CT) data of 75 subjects aged 50 and above who underwent contrast enhanced CT aortograms for various indications at National University Hospital, Singapore (NUH) from 2008 to 2010. Subjects with previous open surgery or endovascular treatment of the thoracic aorta were excluded from the database. The majority (41) of the subjects were Chinese, followed by 10 Malays, 1 Indian, 1 Eurasian and 22 whose ethnicity could not be ascertained as it was not mandatorily recorded.

Geometrical information of the aortas of these six subjects was extracted as axial images (in-plane resolution of 512 by 512 pixels with pixel size of 0.68 mm and slice thickness of 0.6 mm) from our medical CT database. These CT images were imported into Mimics v13.1 (Materialise, Leuven, Belgium)—a medical image processing software, for segmentation and reconstruction of the six subject-specific aortas. These six geometrically variant aortas were segmented semi-automatically from the region distally to the coronary artery to the region proximally to the renal arteries, using Mimics v13.1 (Materialise). Figure 1 displays six geometrically variant models used in the current study. Interestingly, among all the six cases, there is one having a double-curve in the abdominal aorta (Case F).

Meshing and elements

A semi-automatic meshing technique was employed in HyperMesh v10.0 (Altair HyperWorks, Troy, MI, USA) to achieve optimal element quality of the surface meshes. The enclosed regions of the surface meshes were then filled with four-noded tetrahedral elements using the advancing-front method in HyperMesh mesh generator. To optimize between computational efficiency for the transient analysis and accuracy of the result, an average element size of approximately 2 mm was used to mesh the six models, resulting in a range of 500 000–900 000 elements for the six models.

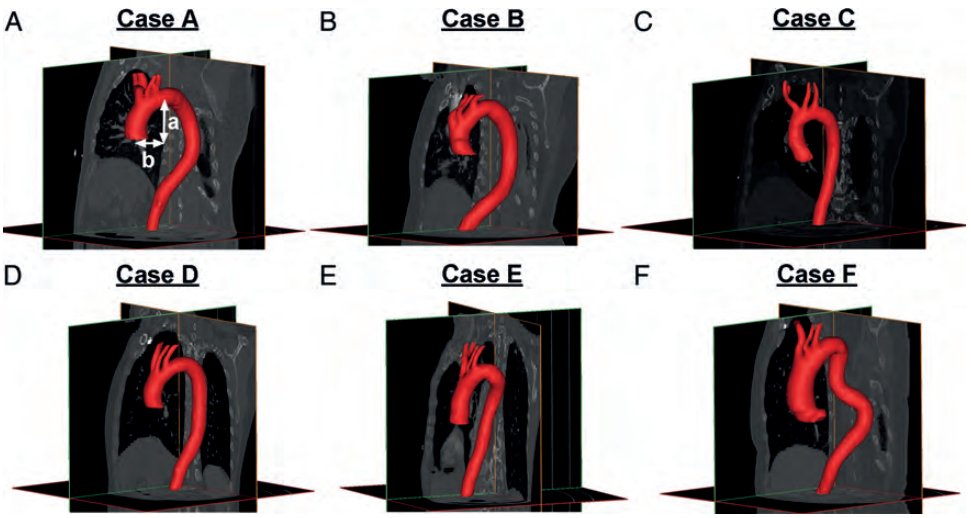

Figure 1: Six subject-specific aorta models with their distinct unique features. (**A**) A 58-year-old subject (aorta arch with large radius of curvature; twisted brachiocephalic artery curving posteriorly). (**B**) A 60-year-old subject (aorta arch with large radius of curvature; supra-aortic arteries curving posteriorly). (**C**) A 57-year-old subject (aorta arch with moderate radius of curvature; bugling brachiocephalic artery curving anteriorly). (**D**) A 54-year-old subject (aorta arch with moderate radius of curvature). (**E**) A 64-year-old subject (aorta arch with very small radius of curvature). (**F**) A 72-year-old subject (S-shaped aorta; dilated bump in both anterior and posterior side of the proximal ascending aorta).

Flow model and boundary conditions

In this study, a commercial finite element package ADINA v8.6.0 (ADINA R&D, Inc., Watertown, MA, USA) was employed for the CFD simulations. Based on textbook references by Fung [7] and other literature [8], blood flow in large vessels is usually assumed to be laminar since the mean flow velocity is predicted to be low enough to result in a relatively low Reynolds number. In our study, the average Reynolds numbers (Re_{ave}) based on the average flow velocity (V_{ave}) and average hydraulic diameter ($D_{h,ave}$) at peak systole ranges from 1249 to 2343 while the maximum Reynolds numbers (Re_{max}) in our models ranges from 1064 to 2389 (Table 1). The average Womersley numbers (α_{ave}) based on the $D_{h,ave}$ ranges from 17.57 to 25.21 (Table 1). For pulsatile unsteady flow, turbulence occurs at a Reynolds number much larger than expected for steady flow due to the fact of a more stable accelerating flow and a more unstable decelerating flow [7]. From the experimental study on canine aortas by Nerem *et al.* [9], critical Reynolds number (Re_c) for unsteady flow takes the form of $Re_c = k\alpha$, with k being the constant of proportionality ranging from 250 to 1000. For our models, Re_c ranges from 4393 to 25 210. Since the Re_{max} for our models are lower than this threshold range of Re_c, the haemodynamic flow in our model was assumed to be laminar [10]. Blood was also assumed to be Newtonian, incompressible and homogeneous [7]. Blood dynamic viscosity and mass density were inputted as 0.00371 Pas and 1060 kg m^{-3}, respectively [11]. The aortic wall was assumed to be rigid and a non-slip condition was applied [8].

Transient analysis was adopted to simulate the pulsatile nature of the blood flow. Time-dependent pulsatile waveforms of flow rate and pressure at the ascending aorta inlet located just above the coronary artery and at the descending aortic outlet respectively, were obtained from Olufsen *et al.*'s work [12] and used as boundary conditions (Fig. 2). These had been verified by various *in vivo* experimental data [7] and were used extensively for both healthy and unhealthy aortas in various numerical simulation works [8, 13]. Each of the three supra-aortic branches, namely, the brachiocephalic artery, left common carotid artery and left subclavian artery was prescribed with 5% of the volume flow rate as determined by an early reported study [14]. These boundary conditions had been used in one of our recently reported studies [6]. The CFD simulation for each model was carried out for four full cycles, such that a time-periodic solution could be obtained [6, 14].

Table 1: Geometrical parameters and flow parameters for the six models at various locations

Model	a (mm)	b (mm)	Curvature ratio (a/b)	Location	Cross-sectional area, A (mm^2)	Cross-sectional perimeter, P (mm)	Hydraulic diameter, D_h[a] (mm)	Average velocity, V_{ave} (mm s^{-1})	Reynolds no., Re[b]	Womersley no., α_{ave}[c]
A	83.68	61.04	1.371	AA	1728.53	147.76	46.79	172.46	2175.22	30.45
				Arch	977.59	111.36	35.11	206.88	1958.07	22.85
				DA	701.95	92.76	30.27	269.17	2196.24	19.70
				Average	1136.02	117.29	38.74	216.17	2257.37	25.21
B	61.76	41.90	1.474	AA	881.39	105.24	33.50	160.46	1448.87	21.80
				Arch	578.55	86.45	26.77	179.61	1295.97	17.42
				DA	486.85	79.91	24.37	206.02	1353.33	15.86
				Average	648.93	90.53	28.67	182.03	1406.75	18.66
C	73.19	33.41	2.190	AA	743.27	95.05	31.28	163.18	1375.80	20.35
				Arch	488.62	78.89	24.77	219.57	1466.19	16.12
				DA	337.89	58.64	23.05	237.58	1476.03	15.00
				Average	523.26	77.53	27.00	206.78	1504.72	17.57
D	62.90	36.34	1.731	AA	749.23	97.50	30.74	144.17	1194.42	20.00
				Arch	508.19	80.47	25.26	204.08	1389.58	16.44
				DA	357.35	55.77	25.63	197.71	1365.95	16.68
				Average	538.26	77.91	27.63	181.99	1355.53	17.98
E	80.28	24.67	3.255	AA	679.63	89.80	30.27	130.37	1063.75	19.70
				Arch	772.57	99.49	31.06	153.15	1282.24	20.21
				DA	236.82	41.94	22.59	192.08	1169.37	14.70
				Average	563.01	77.08	29.22	158.53	1248.50	19.01
F	97.60	27.18	3.591	AA	1474.09	114.31	51.58	171.85	2389.41	33.57
				Arch	605.60	88.84	27.27	197.50	1451.63	17.74
				DA	188.95	48.98	15.43	355.08	1476.98	10.04
				Average	756.21	84.04	35.99	241.48	2342.75	23.42

AA: ascending aorta; DA: descending aorta.

[a] $D_h = \frac{4A}{P}$.

[b] $Re = \frac{V_{ave} D_h}{v}$, where v is the kinematic viscosity in $mm^2\ s^{-1}$.

[c] $c\alpha = \frac{D_h}{2}\left(\frac{\omega}{v}\right)\frac{1}{2}$, where ω is the angular frequency of oscillation.

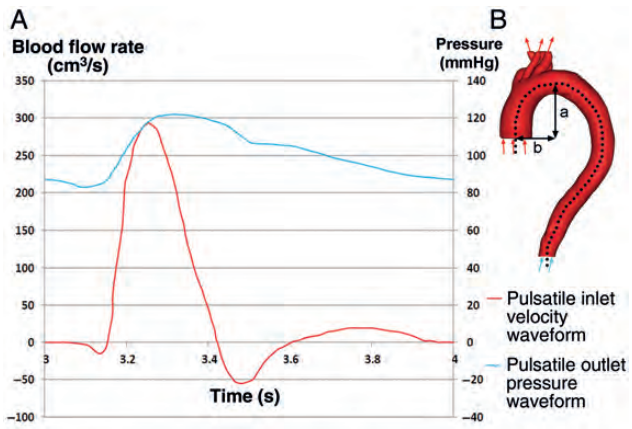

Figure 2: (**A**) Pulsatile inlet flow rate and outlet pressure waveforms. (**B**) Boundary conditions prescribed in the model, with inlet velocity waveform for the aortic inlet and each of the supra-aortic arteries (with 5% of volume flow rate); as well as outlet pressure waveform at the distal descending aorta.

RESULTS

Both ADINA v8.6.0 and EnSight v9.0.3 (Computational Engineering International, Inc., Apex, NC, USA) were used for post-processing. Haemodynamic parameters such as flow pattern and WSS were studied and compared at different cross-sections so as to generate a conclusive observation of haemodynamic behaviours in aortas with distinct geometrical variations.

Flow patterns

Velocity profile. In order to study the aortic flow patterns, axial cross-sectional velocity profiles at various locations, as illustrated in Fig. 3, were captured and compared at specific time instants in the cardiac cycle.

Proximal ascending aorta. Examination of the axial planar velocity flow in the ascending aorta in Case A (Fig. 3A) reveals a parabolic flow profile throughout the cardiac cycle except for the early diastole. This trend is observed in Cases B, C and D as well (Fig. 3B–D). One geometrical similarity among these four cases is the geometrical smoothness of the ascending aorta, unlike the dilated aortic inlet for Cases E and F. Skewed velocity profiles are also noticed in Cases E and F, with their respective skewness towards posterior and anterior wall where the dilated bump is opposite to (Fig. 3E and F).

Distal ascending aorta. The velocity profiles at the distal ascending aorta for Cases A–D are generally axisymmetric in the early and late systoles (Fig. 3A–D). However, they begin to skew towards the inner curvature wall in the peak systole when flow velocity becomes higher (Fig. 3). During peak systole, the velocity profiles in Cases A and C seem to be more skewed with the presence of bulging brachiocephalic artery (Fig. 3A and C). The velocity profiles remain relatively axisymmetric until early diastole when secondary flow develops during flow reversal. For Cases E and F, axisymmetry does not occur in the early and late systoles; in fact, the skewed velocity profiles persist throughout the cardiac cycle (Fig. 3E and F).

Aortic arch. Haemodynamic flow near the aortic arch tends to be disturbed due to a combined effect of complicated geometrical features. Secondary flow continues in aortic arch in Case E in early systole (Fig. 3E). During peak systole, only the velocity profile in Case A resembles a parabola (Fig. 3A), while the rest are axisymmetrically flat with a uniform velocity magnitude. The degree of this parabolicness appears to be associated with the smoothness of the aortic arch; the smoother the arch's transition, the more parabolic the velocity profile. Skewed velocity profiles across the aortic arch section are observed later in the late systole. The skewness towards the inner curvature wall tends to increase with the curvature of the aortic arch (Cases E and F). Non-elliptical or C-shaped regions indicate the continuity of development of secondary flow in the early diastole.

Descending aorta. The flow in descending aortas for Cases A–E is axisymmetrically parabolic during systole period (Fig. 3A–E). The C-shaped velocity region across the axial cross-section can be seen only in the early diastole, especially in Cases A and B where the descending aortas are more inclined away from transverse (or horizontal) plane (Fig. 3). However, the degree of this non-axisymmetry seems to be dependent on the curvature of the descending aorta. For example, the straighter Case E has a relatively parabolic velocity profile across its cross-section. Contrary to all other cases, the flow in double-curved descending aorta (Case F) has noticeable skewness towards its inner curvature wall and outer curvature wall respectively, before and after each bend.

Vortex flow. Figure 4 presents the velocity vector plot of coronal cross-sections of a few cases at various time instants.

Ascending aorta. It can be seen from Fig. 4A that the flow is fairly organized in the ascending aorta of Case B, except during the late systole. Contrary to Case B, vortices are found near the bifurcations of the bugling and twisted brachiocephalic artery of Cases A and C, respectively throughout the cardiac cycle (see supplementary material online). Vortex flow also occurs in the dilated region in the ascending aorta. In Case F, for example, elongated vortices are observed in the dilated region of the ascending aorta (Fig. 4B). These elongated vortices combine with one another, resulting in highly chaotic flow before toning down.

Aortic arch. Figure 4 and Appendix A reveal the presence of vortex flow in the aortic arch of all the cases. This conforms to Kilner *et al.*'s [15] finding using magnetic resonance (MR) velocity mapping as well as Black *et al.*'s [3] and Lam *et al.*'s [13] findings using a numerical approach. In the current study, it is noted that the smoother arches in Cases A and C have a relatively lower-intensified vortices than the sharper arches Case F. Probably due to the flow's incapability of adjusting swiftly to the sudden change in curvature of the aortic arch, substantial local recirculation occurs in the inner curvature distal to the arch during the forward stroke while the outer curvature proximal to the arch experiences the same phenomenon during reversal stroke. This disturbance of flow is exacerbated by the out-of-plane bending of the aorta.

Descending aorta. Despite the expected fairly gentle flow in the straighter descending aorta with lesser variation in geometrical features, the flow in the descending aorta is not undisturbed at all times. Secondary flow is observed in the mid-descending aorta, particularly during the retrograde flow phrases in early systole and late systole. A point to note is that a pair of twin vortices starts to develop near the inner curvature of the descending aorta first, followed by the outer curvature (Fig. 4A). Subsequently, these

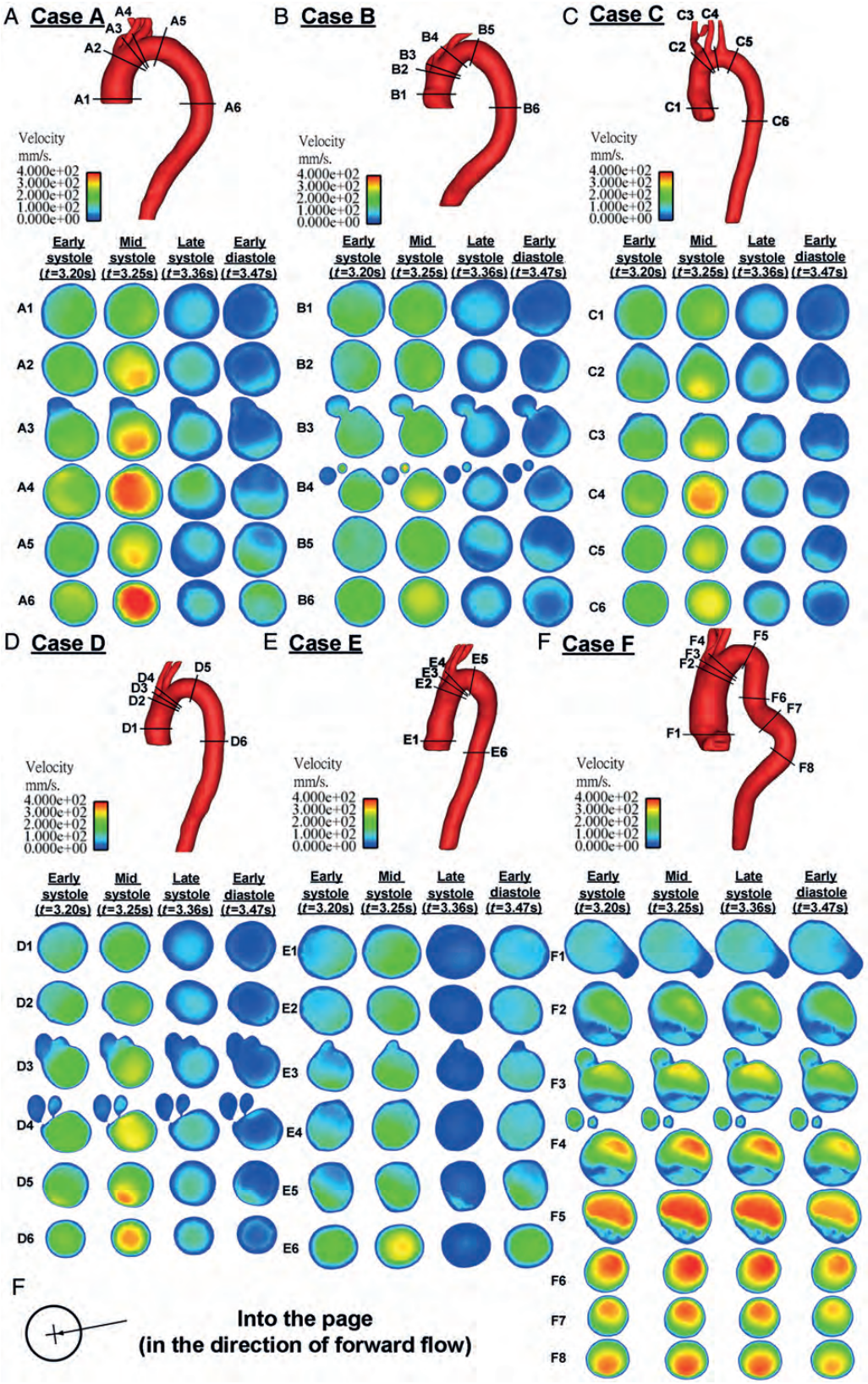

Figure 3: Velocity contour plot of various axial cross-sections of all the six cases at various time instants in the cardiac cycle. (Every cross-section plot has an 'into the page' sign at its centre, indicating that it follows the forward flow direction.)

twin vortices grow in size and propagate to the middle descending aorta. This is a common observation for all cases except Case F, in which vortices develop at the inner curvature wall of each bend, distally to the flow direction (Fig. 4B). This phenomenon conforms to that of the aortic arch when the blood flow is unable to adjust swiftly to the inner curvature after each

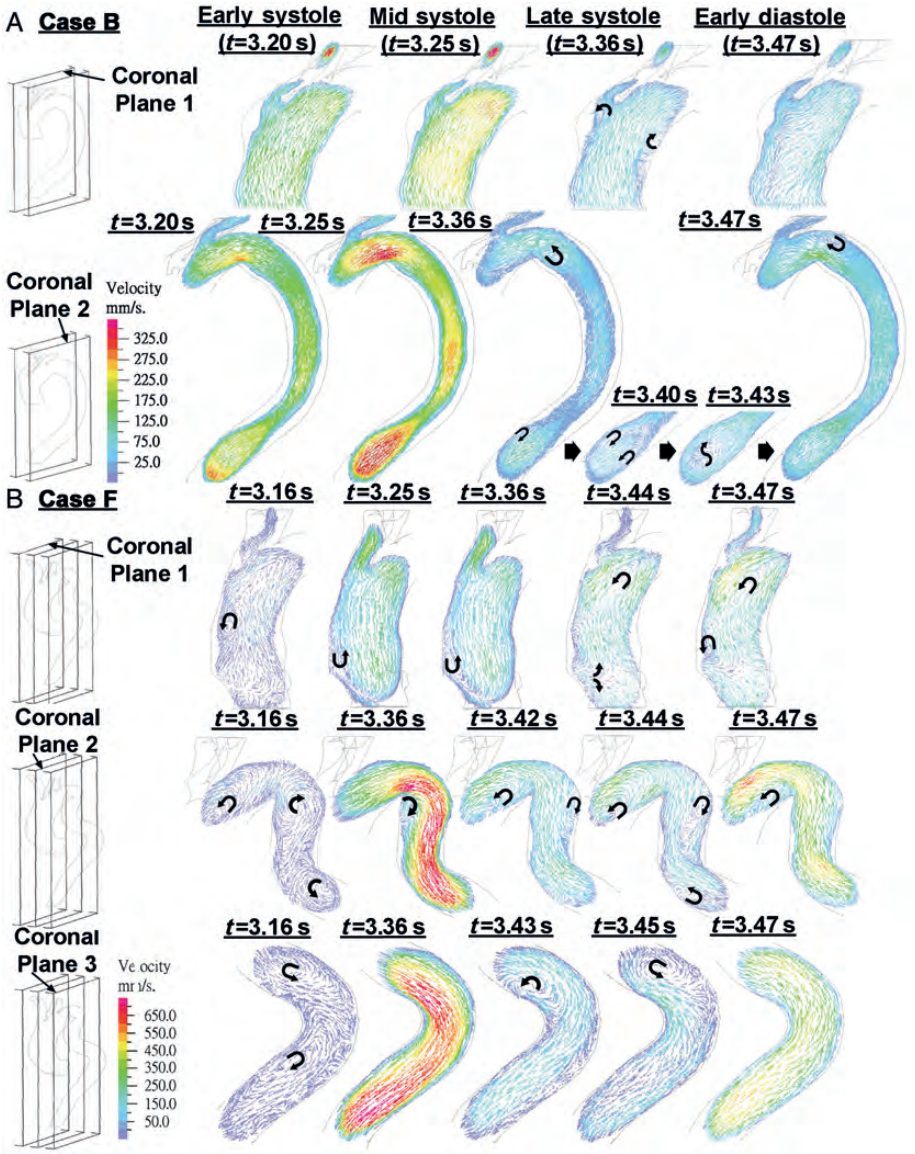

Figure 4: Velocity vector plots of the longitudinal cross-sections of (**A**) Case B and (**B**) Case F at four consecutive critical times in the cardiac cycle. In each case, two cross-sectional planes, labelled as 1 and 2, show the velocity vector plots across the ascending aorta, the aortic arch as well as the descending aorta, respectively.

bend, causing the formation of a local low-velocity region near the inner curvature. The cumulative effect of two simultaneous bends in different planes accentuates the disorder of flow.

Helical flow. Figure 5 displays the streamline plots at different time instant of the fourth cardiac cycle. For all cases, the streamline plots at early systole and mid systole are essentially undistinguishable. Helical flow is most prevalent from the proximal ascending aorta to the distal aortic arch, for Cases A–E. Two types of helical flow are observed: left-handed (or clockwise) rotation and right-handed (or anticlockwise) rotation. The left-handed rotation diminishes when the flow approaches the aortic arch. On the other hand, the right-handed rotation persists even after the aortic arch. This observation is consistent with Morbiducci *et al.*'s [5] results. Case F exhibits a slightly different trend, as an additional minor helical flow of left-handed rotation existed in the descending aorta together with right-handed rotation. This anomaly is hypothesized to be a consequence of Case F's eccentric shape. Among all the models, a helical flow is always observed in the ascending aorta at all time instants. The intensity of the helical flow starts to diminish at late systole, particularly in Cases A, B and E where the helical flow completely vanishes.

Wall shear stress

WSS, which cannot be measured directly by current *in vivo* techniques, can be determined from CFD by calculating the gradient of the velocity field. However, a better representative of WSS over a cardiac cycle is the time-averaged WSS (TAWSS). The distribution and lowest dip of TAWSS for the cases are shown in Fig. 6 and Table 2, respectively. It can be seen that the descending aorta generally tends to have higher TAWSS than the ascending aorta. This is because TAWSS is generally higher in regions where flow is less disturbed and fluent and lower in regions where flow is more disturbed and of lower velocity. Apparently, in most of the cases, the lowest TAWSS of around 25–33 mPa

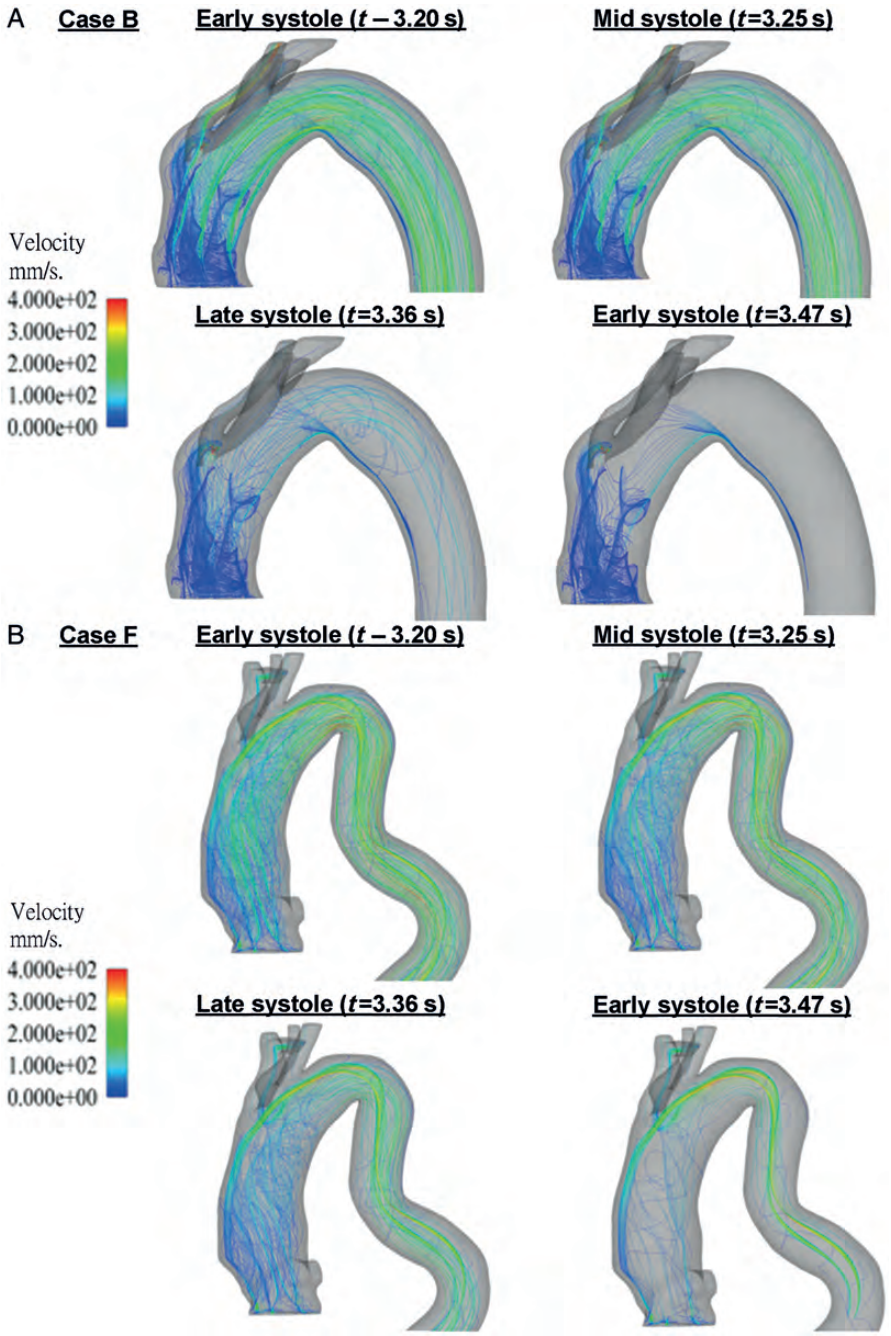

Figure 5: Streamline plot depicting streamlines from the randomly selected node at the aortic inlet in both (**A**) Case B and (**B**) Case F during the early systole (t = 3.20 s); the mid-systole (t = 3.25 s); the late systole (t = 3.36 s) and the early diastole (t = 3.47 s).

occurs in branchiocephalic artery, its sub-branches, right subclavian and right common arteries, as well as left subclavian artery (Fig. 6 and Table 2). The only exception is Case F with its lowest TAWSS in the dilated bump at the left-posterior region of the proximal ascending aorta where the disturbed vortex occurs. Moreover, the left common carotid artery apparently experiences lower TAWSS when compared with the other supra-aortic arteries. Regions of relative low TAWSS are also mainly found near the orifices of supra-aortic branches and ascending aorta. Interestingly, slightly lower TAWSS is also noted in the outer curvature wall of the aortic arch than its inner curvature despite the presence of secondary flow in the inner curvature during the forward stroke dominating the cardiac cycle. Besides the aortic arch, a similar observation is found in the S-shaped Case F, where the outer curvature wall near the two consecutive bends experiences a slightly lower TAWSS.

DISCUSSION

Effect of aortic morphology on haemodynamics and developing pathobiology of cardiovascular diseases

Intricate local geometrical features of the human aorta have a profound effect on haemodynamics. Due to the considerable

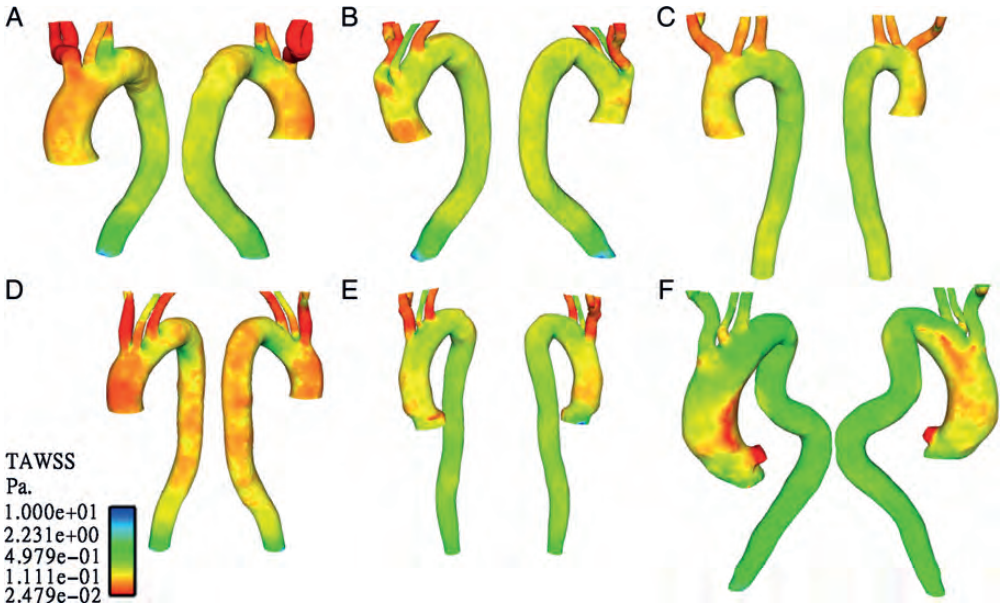

Figure 6: TAWSS contour plots on the surface of (**A**) Case A, (**B**) Case B, (**C**) Case C, (**D**) Case D, (**E**) Case E and (**F**) Case F. For each case, left hand side shows the right-anterior view of the aorta while right shows the left-posterior view. (TAWSS scale increases exponentially to show the unevenly distribution of TAWSS.)

Table 2: Time-averaged WSS for the six models

Case	Region of min. TAWSS	Min. TAWSS (Pa)	Mean TAWSS over the following regions (Pa)				
			PAA	DAA	AA	PDA	DDA
A	Brachiocephalic artery, right subclavian artery, right common carotid artery	2.48E–02	7.98E–02	7.12E–02	1.15E–01	1.03E–01	4.02E–01
B	Brachiocephalic artery, right subclavian artery, right common carotid artery, left subclavian artery	2.56E–02	6.50E–02	9.37E–02	1.35E–01	1.51E–01	4.43E–01
C	Brachiocephalic artery, right subclavian artery, right common carotid artery	3.11E–02	8.57E–02	1.03E–01	2.96E–01	2.12E–01	2.36E–01
D	Brachiocephalic artery, right subclavian artery, right common carotid artery, left subclavian artery	2.53E–02	4.85E–02	7.24E–02	1.23E–01	8.25E–02	2.56E–01
E	Brachiocephalic artery, right subclavian artery, right common carotid artery, left subclavian artery	2.77E–02	9.24E–02	1.78E–01	2.48E–01	2.13E–01	3.91E–01
F	Proximal posterior ascending aorta	3.26E–02	5.90E–02	9.01E–02	3.35E–01	4.69E–01	4.89E–01

PAA: proximal ascending aorta; DAA: distal ascending aorta; AA: aortic arch; PDA: proximal descending aorta; DDA: distal descending aorta.

anatomical distortions present in each model, the blood flow in aortas is rather disturbed and substantial recirculation is observed.

In our study, it is found that the irregular contour of the aortic wall causes disturbance in the flow pattern. Skewed flow profiles are mainly found in regions where there is abrupt change in the cross-section area, with the tendency to skew towards the opposite side of a dilated region. Additionally, the contouring of the supra-aortic arteries seems to have some influence on skewness of velocity profiles in the distal ascending aorta; the more bulging the supra-aortic arteries are, the higher the degree of skewness would be. The flow profiles in the aortic arch or bends are generally skewed towards the inner curvature wall, and this is consistent with Batten and Nerem's [16] measured result. This skewed flow gives rise to the formation of low-velocity regions where secondary flow occurs. Additionally, our study shows that the skewness towards the inner curvature wall tends to increase with the curvature of the aortic arch.

Vortex flow is prevalent, especially during retrograde flow phases in early and late systole. This is in good agreement with Matsumoto *et al.*'s [17] finding using tagging cine MR. Due to lid-driven cavity effect [18], a sudden increase in cross-sectional area in the ascending aorta (i.e. aortic dilation) is expected to predispose to flow separation. A significant amount of vortex flow also develops at the inner curvature of the aortic arch during forward stroke and at the outer curvature of the arch during the return stroke. A similar vortical flow pattern was also observed in MR velocity mapping study by Kilner *et al.* [15], which validates our qualitative results. Moreover, in our study, it is observed that high-velocity vortices tend to form in the distal aortic arch with increasing curvature. This is in accordance with Naruse and Tanishita's [19] experimental findings. Such disturbance in intra-aortic flow, even in healthy subjects, may have significant relation to the pathogenesis of atheroma in the aortic arch [15]. Our study also shows that a pair of twin vortices in mid-descending aorta stems from the inner curvature wall first,

followed by the outer curvature wall, and subsequently propagates to the middle line before merging up as fluent flow.

In addition, a helical flow is observed in the ascending aortas using streamline plots, and this confirms Zabielski and Mestel's [20] as well as Kilner *et al.*'s [15] findings. It is interesting to note that a small degree of helical flow presents in the S-shaped descending aorta (Case F), suggesting a possibility of geometrical influence, other than the pulsatile nature of blood, on helical flow.

WSS, which plays a major role in the generation, progression and destabilization of atherosclerotic plaque, may have important therapeutic implications in atherosclerosis development [21]. Gnasso *et al.*'s [22] clinical observation showed that lower WSS was associated with plaque in atherosclerosis. In fact, various studies had reported that low WSS increased the expression of E-selectin and adhesion molecules that favour the recruitment of plaque to intima [23]. Surprisingly, despite the presence of secondary flow in the inner curvature dominating the cardiac cycle during the forward stroke, the low-velocity flow during the reversal stroke causes the outer curvature wall of the aortic arch to experience slightly lower TAWSS than its inner curvature wall. In other words, WSS depends on both the magnitude and angle of the velocity vector at the wall; WSS is generally higher in regions where flow is fluent and parallel to the aortic wall and lower in regions where secondary flow occurs. Regions of relative low TAWSS are mainly found in the ascending aorta, for example, around the orifices of supra-aortic branches, the common carotid arteries as well as the outer curvature wall of aortic arch. These coincide with the predilection sites for atherosclerosis reported by literature [24].

LIMITATIONS

Similar to any other computational study, our work made a number of simplifications and assumptions. The aortic wall dynamics, which are highly dependent on the elasticity of the aortic wall, was not simulated in our study. The elastic aortic wall experiences rapid deformation throughout the cardiac cycle and this may cause local effects on haemodynamics. Nevertheless, as suggested by Hoi *et al.* [25], the effects of aortic wall dynamics may be of secondary order to the distinct aortic anatomy. Moreover, the variation in the average aortic size in the entire cardiac cycle is considered as minimal and less significant. The present study made this customary assumption of a rigid aortic wall since the incorporation of aortic wall dynamics poses technical challenges in qualifying the spatial and temporal deformation in these small and complex vessels [25]. However, with advances in computational technologies, the incorporation of aortic wall dynamics would be needed in future study. Another assumption would be the non-subject specific boundary conditions taken from the published work of Olufsen *et al.* [12]. There are reported works [25] using subject-specific flow conditions for a more accurate prediction of cardiovacular pathology. However, it should be highlighted that it would be inappropriate to use different subject-specific flow conditions in our comparison study.

CONCLUSIONS

As known previously [21], aortic morphology plays a key role in determining the nature of the haemodynamic pattern, with mutual association between both the former and the latter, which in turns relates to the development of vascular diseases. In the present study, a general trend of haemodynamic behaviours associated with various local geometrical features has been identified. Secondary flow such as vortices, helix and skewness of flow profile, which associates with low WSS, is common in the aorta with irregular contour, numerous bends, bulging supra-aortic branches and large degree of curvature at its arch. Combining with the known correlation between haemodynamics and the underlying risks in the development of cardiovascular diseases, our study hopes to provide a better understanding of the relationship between aortic morphology and developing pathobiology of vascular diseases.

SUPPLEMENTARY MATERIAL

Supplementary material is available at *EJCTS* online.

ACKNOWLEDGEMENTS

We would like to thank the Department of Diagnostic Imaging of the National University Hospital (NUH), Singapore for providing the medical CT images.

Conflict of interest: none declared.

REFERENCES

[1] Vasava P, Dabagh M, Jalali P. Effect of aortic arch geometry on pulsatile blood flow: flow pattern and wall shear stress. In: Dössel O, Schlegel WC (eds). World Congress on Medical Physics and Biomedical Engineering. September 7–12, 2009. Munich, Germany: Springer, 2009. p. 1206–9.
[2] Rayz VL, Berger SA. Computational modeling of vascular hemodynamics. In: De S, Guilak F, Mofrad RKM (eds). Computational Modeling in Biomechanics. New York: Springer, 2010.
[3] Black MM, Hose DR, Lawford PV. The origin and significance of secondary flows in the aortic arch. J Med Eng Technol 1995;19:192–7.
[4] Morrison TM, Choi G, Zarins CK, Taylor CA. Circumferential and longitudinal cyclic strain of the human thoracic aorta: age-related changes. J Vasc Surg 2009;49:1029–36.
[5] Morbiducci U, Ponzini R, Rizzo G, Cadioli M, Esposito A, Cobelli FD *et al.* In vivo quantification of helical blood flow in human aorta by time-resolved three-dimensional cine phase contrast magnetic resonance imaging. Ann Biomed Eng 2009;97:516–31.
[6] Tse KM, Chiu P, Lee HP, Ho P. Investigation of hemodynamics in the development of dissecting aneurysm within patient-specific dissecting aneurismal aortas using computational fluid dynamics (CFD) simulations. J Biomech 2011;44:827–36.
[7] Fung YC. Biomechanics: Circulation, 2nd edn. New York: Springer, 1997.
[8] Cheng SW, Lam ES, Fung GS, Ho P, Ting AC, Chow KW. A computational fluid dynamic study of stent graft remodeling after endovascular repair of thoracic aortic dissections. J Vasc Surg 2008;48:303–9.
[9] Nerem RM, Seed WA, Wood NB. An experimental study of the velocity distribution and transition to turbulence in the aorta. J Fluid Mech 1972; 52:137–60.
[10] Morris L, Delassus P, Callanan A, Walsh M, Wallis F, Grace P *et al.* 3-D numerical simulation of blood flow through models of the human aorta. J Biomech Eng 2005;127:767–75.
[11] Paul MC, Molla MM, Roditi G. Large-Eddy simulation of pulsatile blood flow. Med Eng Phys 2009;31:153–9.
[12] Olufsen MS, Peskin CS, Kim WY, Pedersen EM, Nadim A, Larsen J. Numerical simulation and experimental validation of blood flow in arteries with structured-tree outflow conditions. Ann Biomed Eng 2000;28:1281–99.
[13] Lam SK, Fung GS, Cheng SW, Chow KW. A computational study on the biomechanical factors related to stent-graft models in the thoracic aorta. Med Biol Eng Comput 2008;46:1129–38.

[14] Shahcheraghi N, Dwyer HA, Cheer AY, Barakat AI, Rutaganira T. Unsteady and three-dimensional simulation of blood flow in the human aortic arch. J Biomech Eng 2002;124:378–87.
[15] Kilner PJ, Yang GZ, Mohiaddin RH, Firmin DN, Longmore DB. Helical and retrograde secondary flow patterns in the aortic arch studied by three-directional magnetic resonance velocity mapping. Circulation 1993;88(5 Pt 1):2235–47.
[16] Batten JR, Nerem RM. Model study of flow in curved and planar arterial bifurcations. Cardiovasc Res 1982;16:178–86.
[17] Matsumoto Y, Honda T, Hamada M, Toyama T, Matsuoka H, Hiwada K. Evaluation of short axial blood flow pattern in thoracic descending aorta by use of tagging cine magnetic resonance. Angiology 1994;45:917–22.
[18] Mercan H, Atalik K. Vortex formation in lid-driven arc-shape cavity flows at high Reynolds numbers. Eur J Mech B Fluids 2009;28:61–71.
[19] Naruse T, Tanishita K. Large curvature effect on pulsatile entrance flow in a curved tube: model experiment simulating blood flow in an aortic arch. J Biomech Eng 1996;118:180–6.
[20] Zabielski L, Mestel AJ. Helical flow around arterial bends for varying body mass. J Biomech Eng 2000;122:135–42.
[21] Friedman M, Giddens D. Blood flow in major blood vessels—modeling and experiments. Ann Biomed Eng 2005;33:1710–3.
[22] Gnasso A, Irace C, Carallo C, De Franceschi MS, Motti C, Mattioli PL et al. In vivo association between low wall shear stress and plaque in subjects with asymmetrical carotid atherosclerosis. Stroke 1997;28:993–8.
[23] Slager CJ, Wentzel JJ, Gijsen FJH, Schuurbiers JCH, van der Wal AC, van der Steen AFW et al. The role of shear stress in the generation of rupture-prone vulnerable plaques. Nat Clin Pract Cardiovasc Med 2005;2:401–7.
[24] Dhawan SS, Avati Nanjundappa RP, Branch JR, Taylor WR, Quyyumi AA, Jo H et al. Shear stress and plaque development. Expert Rev Cardiovasc Ther 2010;8:545–56.
[25] Hoi Y, Zhou YQ, Zhang X, Henkelman RM, Steinman DA. Correlation between local hemodynamics and lesion distribution in a novel aortic regurgitation murine model of atherosclerosis. Ann Biomed Eng 2011;39:1414–22.

European Journal of Cardio-Thoracic Surgery 43 (2013) 838–839
doi:10.1093/ejcts/ezs469 Advance Access publication 21 August 2012

EDITORIAL COMMENT

Correlate blood pressure, not blood flow, with atherosclerosis

Mano J. Thubrikar*

Thubrikar Aortic Valve, Inc., Rapid City, SD, USA

* Corresponding author. Thubrikar Aortic Valve, Inc. 525 University Loop, Suite 105, Rapid City, SD 57701, USA. Tel: +1-714-8330383; fax: +1-714-6937851; e-mail: mano.thubrikar@hotmail.com (M.J. Thubrikar).

Keywords: Atherosclerosis • Vascular mechanics • Haemodynamics

Over the last 50 years, there have been extensive studies on fluid dynamics in the aorta and arteries and they have included both experimental measurements as well as computational modelling. Almost always, these studies have been carried out to suggest that the arterial pathology, particularly atherosclerosis, is a result of some parameters of haemodynamics. As the computational and flow measurement techniques become better with time, the data obtained have become more precise as well as more data have been obtained. The paper for which these comments are written [1] represents this type of advance in the study of haemodynamics.

The term 'haemodynamics' means 'blood flow' (haem = blood, dynamics = motion or flow, in this case). I have always maintained that blood flow does not relate to the genesis of atherosclerosis. Unfortunately, large numbers of papers are written in this area and that makes more people want to believe in this concept, whether it is correct or not. More work on haemodynamics in fact discourages the development of alternative concepts.

There are reasons to believe that another concept based on the effect of arterial blood pressure 'arterial mechanics, that determines arterial stresses and strains' relates to the genesis of atherosclerosis [2]. In reference [2], there are descriptions that establish the following correlations: (1) an atheroma forms at the sites of stress concentration; (2) sites of reduced wall stress are the sites of atheroma inhibition; (3) an increase in arterial pressure increases wall stress and also increases atherosclerosis; (4) a decrease in heart rate (such as by beta-blockers or by other means) decreases cyclic stress and cyclic strain over a given period of time and also decreases atherosclerosis; etc.

No such clear correlation exists between haemodynamics and atherosclerosis in spite of several decades of research in this subject. In the past, attempts were made to correlate haemodynamic parameters such as high shear, low shear and oscillating shear stress to the formation of atherosclerosis. In the present paper, yet another haemodynamic parameter 'secondary flow' has been implicated in the formation of atheromas. The paper has also described several haemodynamic parameters as follows: (1) skewed velocity profile; (2) vortex flow; (3) chaotic flow; (4) flow reversal; (5) secondary flow; (6) helical flow; (7) time-averaged wall shear stress and (8) combinations of these. It is obvious that changes in the geometry create changes in haemodynamics.

The authors have done an excellent job of taking the aortas of patients and choosing the aortas of differing geometries for their studies to understand the larger differences in haemodynamics. They have also done an excellent job of the computational analysis of flow and relating that to the changes in the geometry. One would expect that the haemodynamic changes secondary to geometry changes could have an effect on processes like platelet aggregation and/or thrombus formation. However, such a correlation is yet to be established. The study presented has its own merit even though, in my opinion, haemodynamic